Paper II

JOURNAL OF PHYSICAL ORGANIC CHEMISTRY
J. Phys. Org. Chem. 2006; **19:** 25–33
Published online 17 October 2005 in Wiley InterScience (www.interscience.wiley.com). DOI: 10.1002/poc.990

Catalytic dehydrogenation of ethane over mononuclear Cr(III)–silica surface sites. Part 2: C—H activation by oxidative addition

Sindre Lillehaug, Vidar R. Jensen and Knut J. Børve*

Department of Chemistry, University of Bergen, Allégaten 41, NO-5007 Bergen, Norway

Received 20 April 2005; revised 1 August 2005; accepted 3 August 2005

ABSTRACT: Models of Cr(III)–silica were used to study C—H activation in ethane by oxidative addition as a possible route to catalytic dehydrogenation. This mechanism involves a formal double oxidation of chromium and a minimum energy crossing point (MECP) was located on the seam between the quartet spin potential energy surface of Cr(III) and the doublet spin potential energy surface of Cr(V). Subsequent to the change of spin state, the C—H activation path passes through a transition state on the doublet potential surface, leading to the formation of an ethylhydridochromium(V) complex. This complex represents only a shallow minimum on the potential energy surface and β-hydrogen transfer to complete the catalytic cycle must therefore take place in the extension of the C—H activation step. The combination of a significant activation energy and a small pre-exponential factor in the rate constant makes C—H activation by oxidative addition an unlikely mechanism for dehydrogenation in this system.

KEYWORDS: Cr–silica; ethane; C—H activation; minimum energy crossing point; dehydrogenation; density functional theory; cluster; catalysis

INTRODUCTION

A proven catalyst for the dehydrogenation of short alkanes, Cr–oxide systems have been a topic of research since 1933.[1] This effort has provided significant insight through a variety of experimental designs.[2] The dominant view in the modern literature is that chromium(III) is the oxidation state showing the highest activity for dehydrogenation, possibly with minor contributions from the +II state.[3–8] *In situ* diffuse-reflectance UV–visible spectroscopy (DRS) has been used to establish a semi-quantitative relationship between the number of pseudo-octahedral Cr(III) sites on mixed alumina–silica supports and dehydrogenation activity.[3] Combined reactivity and characterization studies of Cr–silica[4,9] led DeRossi *et al.*[4] to propose the catalytically active chromium species to be bonded to the surface via two oxygen bridges and with hydroxyl as the third ligand, cf. Fig. 1.[4] From its spectroscopic signature, this species was dubbed $Cr^{III}G$.

Owing to the complexity of the catalyst surface, much about the active site and the reaction mechanism is still unknown. One crucial question concerns the mechanism of C—H activation, for which the focus has been on activation through direct interaction with chromium.[10] The mechanistic information available is scarce. An attractive strategy is therefore to consider, systematically, the different C—H activation mechanisms known from organometallic chemistry. The two most relevant ones are oxidative and electrophilic addition.[11] Electrophilic addition is also known as σ-bond metathesis,[12] since metal–ligand and C—H bonds are replaced by metal–carbon and ligand–hydrogen bonds. Conversely, in oxidative addition of ethane, carbon and hydrogen bind directly to the metal as the C—H bond is broken. This involves a formal oxidation of the metal and a change of spin state. Owing to spin–orbit coupling, the reaction may proceed on a single adiabatic potential energy surface corresponding to the full electronic Hamiltonian. A reaction scheme involving spin flip in the course of the reaction is known as 'two-state reactivity' (TSR).[13] The role of TSR in C—H activation and other transition metal-catalysed reactions, has recently been reviewed.[14]

In general, σ-bond metathesis is favoured on light, electron-deficient metals, whereas oxidative addition is favoured on the heavy and electron-rich late transition metals.[15–18] There are exceptions to this rule,[12,19,20] and although chromium is a first-row transition metal, oxidative addition cannot be ruled out *a priori*. For instance, oxidative addition has been found feasible on O═Cr═O and Cr═O.[21] Furthermore, H_2 activation by oxidative addition has been reported for a Cr(III) complex with

**Correspondence to:* K. J. Børve, Department of Chemistry, University of Bergen, Allégaten 41, NO-5007 Bergen, Norway.
E-mail: knut.borve@kj.uib.no
Contract/grant sponsor: Research Council of Norway (NFR); *Contract/grant number:* KOSK 141953 431.

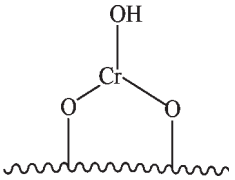

Figure 1. The $Cr^{III}G$ structure proposed to be active in dehydrogenation of alkanes[4]

three ligands covalently bonded through nitrogen.[22] This complex is similar in essence to the $Cr^{III}G$ species proposed as active in dehydrogenation by DeRossi *et al.*[4]

In a previous study, we explored C—H activation by σ-bond metathesis in the Cr–oxide system.[23] Following proposals in the literature,[2,24] a mechanism was studied that involves activation and reformation of a Cr—O bond on chromium species that are stabilized by three oxygen ligands. However, the computed activation energy exceeds $200\,kJ\,mol^{-1}$ and seems prohibitively high for catalytic activity. Significantly lower activation energy was found for an alternative mechanism in which C—H activation takes place at a reactive hydridochromium surface species. The importance of the latter mechanism relies on the ability of the chromium site to stabilize the hydride, which is reactive with respect to formation of a Cr—O bond in the vicinity of hydroxyl species. Alternative routes to C—H activation should therefore be explored.

Here, we investigated whether C—H activation by oxidative addition may represent a viable route to alkane dehydrogenation. As in Ref. 23, we studied the Cr–silica model catalyst, taking the $Cr^{III}G$ structure in Fig. 1 as our starting point and exploring the more general, conceptual model of mononuclear Cr(III) complexes with three covalent ligands coordinating through oxygen. The importance of the choice of oxide carrier for the catalytic dehydrogenation reaction is the subject of a forthcoming publication [25].

COMPUTATIONAL DETAILS

Models and methods

The surface models used in the current study are detailed in Ref. 23. Cluster models were constructed either in an *ad hoc* manner, drawing on chemical intuition and experimental facts or systematically, starting from low-index surfaces of silica crystals.

The *ad hoc* models include a generic model of the $Cr^{III}G$ species as proposed by DeRossi *et al.*[4] The silica surface is represented by a disiloxy ether moiety and the model is denoted by *gen-2bridge*, cf. Fig. 2(A). To model a site completely void of surface constraints yet having a first coordination sphere similar to that of the $Cr^{III}G$ species, the $Cr(OH)_3$ molecule is used, Fig. 2(B).

Improved models taking into account larger parts of the amorphous oxide carrier have been generated from low-index surfaces of the high-T modifications of silica,

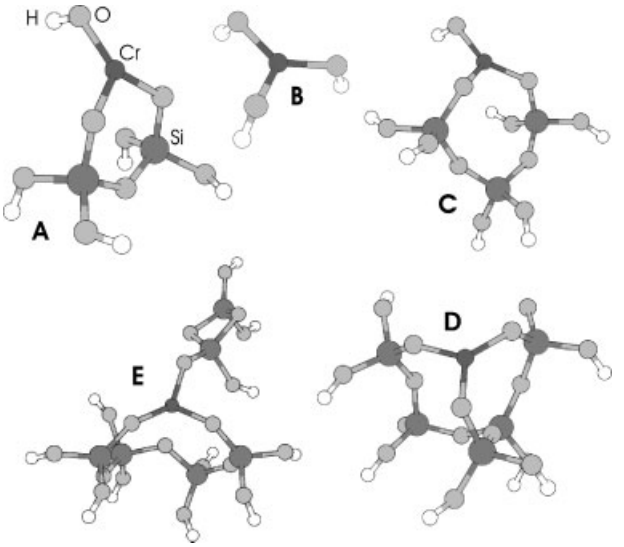

Figure 2. Cluster models of Cr(III)–silica surface sites: *gen-2bridge* (A), $Cr(OH)_3$ (B), *(100)-2bridge* (C), *(101)-3bridge* (D) and *(111)-3bridge* (E)

α- and β-cristobalite.[23] On each surface, a cluster region was defined that includes chromium and its local chemical environment, with boundary bonds $O_{cluster}$–Si_{host} severed and terminated by hydrogen atoms. In this work, the models have been applied only as isolated clusters, cf. the *(100)-2bridge*, *(111)-3bridge* and *(101)-3bridge* models in Fig. 2(C), (D) and (E), respectively.

Mimicking the restoring forces of the extended structures, atoms at the cluster boundaries have their positions fixed to those of the parent slab model. In the two-bridge models, this implies frozen position for all atoms but those of the $(—O)_2CrOH$ moiety. In the three-bridge models, the terminating $Si(OH)_n$ groups were held in fixed positions.

Quantum mechanical (QM) calculations were performed using density functional theory as implemented in the Amsterdam Density Functional (ADF) set of programs.[26–28] For electron correlation the LDA functional of Vosko *et al.*[29] augmented by the non-local 1986 corrections by Perdew[30] were used. The exchange functional consists of the Slater term augmented by gradient corrections as specified by Becke.[31] For details of basis sets and geometry optimisation, see Ref. 23.

In general, energy differences refer to electronic degrees of freedom only, i.e. without zero-point vibrational energies or temperature effects. In order to take into account temperature and entropy effects, the full set of thermodynamic functions were computed in the harmonic and rigid-rotor approximation for simulations based on the *gen-2bridge* surface model. The numerical integration schemes were used with the tightest accuracy request available. All stationary structures display an ultra-soft vibrational mode which consistently has been omitted from the harmonic analysis.

Minimum energy crossing points (MECPs) between spin potential energy surfaces were optimized using ADF, in

conjunction with the code developed by Harvey and coworkers.[32,33] A set of shell scripts and Fortran programs were used to extract energies and gradients for the two spin states and to combine these to produce an effective gradient pointing toward the MECP and used to update the geometry. The convergence criteria are energy difference <0.1 mhartree and a gradient at the seam of crossing within the normal ADF convergence criterion. Subsequent frequency analysis used the effective Hessian[32] along the hyperline of equal energy of the two potential energy surfaces. The unix scripts and Fortran programs were adapted to ADF in the course of this work.

Accuracy

To compare the one- and two-state mechanisms of dehydrogenation, initiated by σ-bond metathesis and oxidative addition, respectively, the accuracy of the applied density functional method should be considered, in particular with respect to the relative stability of the two spin states involved in the oxidative addition. Relative energies computed on a single potential surface are generally in agreement with more sophisticated methods,[34–37] whereas prediction of relative energies on different potential surfaces is more problematic.[38,39] Poli and Harvey[38] reported that 'pure' density functionals such as BP86 tend to exaggerate the stability of low-spin forms, whereas hybrid functionals such as B3LYP may overestimate the stability of high-spin species. Accordingly, in a study of the Cr—OH bond dissociation energy (BDE) in oxohydroxylchromium complexes with oxidation states I–VI, the pure BPW91 and hybrid B3LYP functionals reproduced the general trend of more sophisticated methods, but over- and underestimated, respectively, the BDE at higher oxidation states.[40] Moreover, BPW91 systematically but modestly overestimated the stability of doublet states relative to quartet states in the insertion reaction of ethene in $[H(NH_3)Cr^{III}Me]^+$.[41] BP86 as applied here might therefore be expected to underestimate the activation energy for the two-state mechanism involving oxidative addition relative to that of the one-state mechanism involving σ-bond metathesis. An indication of this was obtained using the Gaussian set of programs[42] to compute the quartet/doublet energy difference of the $Cr(OH)_3$ model. In line with the pattern described above, B3LYP puts the low-spin doublet 116 kJ mol^{-1} above the high-spin quartet, while a difference of 75 kJ mol^{-1} was obtained using BP86 in both ADF and Gaussian. At any rate, differences <20 kJ mol^{-1} in relative energies computed for different reaction paths are considered to be within the error bars of the method.

RESULTS

We start out by exploring C—H activation by oxidative addition, followed by constructing a complete mechanism of dehydrogenation. For convenience, each chromium site is referred to by the ligands in the first coordination sphere of the metal. For instance, a general DeRossi-type site may be denoted by $(—O)_2CrOH$, where —O represents a generic oxygen ligand singly bonded to chromium.

C—H activation

Ethane is found not to form any molecular complex with chromium on DeRossi-type Cr(III) sites.[23] This implies that the initial encounter is reactive rather than physisorptive. The reaction path of oxidative addition (OA) is first presented as computed for the *gen-2bridge* cluster model [Fig. 2(A)]. In the unreacted cluster the coordination geometry of chromium is trigonal planar. The ground state has quartet spin multiplicity, the doublet being higher in energy by 75 kJ mol^{-1}. A schematic representation of the electronic energy profile of C—H activation by oxidative addition is presented in Fig. 3, together with geometries of important stationary structures. As ethane approaches chromium, one of the C—H bonds stretches and the energy increases on both spin surfaces. The gradient is larger on the quartet surface and the first step towards OA is thus crossing from the quartet to the doublet potential energy surface at an MECP. The MECP

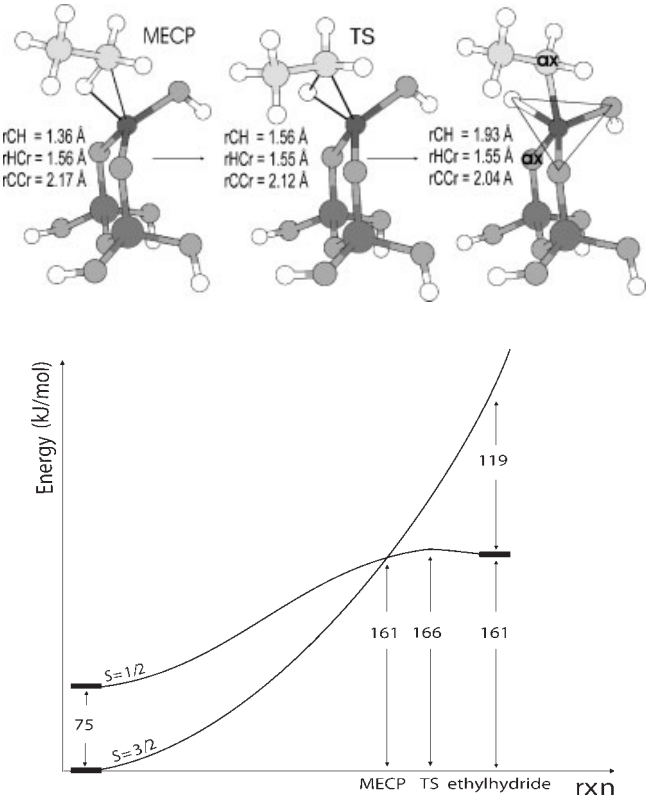

Figure 3. Geometric parameters (top) and schematic representation of the electronic energy profile (bottom) for C—H activation by oxidative addition on the *gen-2bridge* model to form an ethylhydridochromium(V) complex

was located at an activated C—H bond length of rCH = 1.36 Å and with the active hydrogen atom starting to displace a bridging oxygen from the equatorial plane toward an axial position in the trigonal bipyramidal coordination geometry, cf. Fig. 3.

Frequency analysis at the MECP gives an imaginary frequency in excess of $900i\,\mathrm{cm}^{-1}$ corresponding to the reaction coordinate orthogonal to the seam of crossing. After removal of this component, an imaginary frequency of about $5i\,\mathrm{cm}^{-1}$ remains, probably due to numerical noise. At the MECP, the spin density on chromium drops from 2.8 in the quartet to 1.1 in the doublet state. The electronic effects of spin change are localized to chromium, leaving all Mulliken atomic charges essentially unaffected.

Past the MECP and now on the doublet potential surface, the C—H bond continues to lengthen while the energy increases slowly, until a transition state (TS) is reached at rCH = 1.56 Å, cf. Fig. 3. The Cr–H distance remains essentially constant from the MECP through the transition state and to the product complex. The coordination geometry of the resulting ethylhydridochromium(V) complex may be described as a pseudo-trigonal bipyramid, although the widest angle is only 140°. Together with the fact that the energy changes only slightly after the MECP (see Table 1), the geometry changes just described are consistent with a late transition state. Most of the C—H activation and all of the Cr—H bond formation takes place in the quartet state. Past the MECP, the energy cost of completing the rupture of the C—H bond seems to be compensated for by the formation of the C—Cr bond.

At 500 °C, the enthalpy and Gibbs free energy of C—H activation are computed as 162 and 283 kJ mol^{-1}, respectively (cf. Table 1). The large contribution from entropy is due to the loss of translational and rotational degrees of freedom when reducing the molecularity. The change in electronic energy agrees well with that of the enthalpy.

The corresponding reactions on the $Cr(OH)_3$ and *(100)-2bridge* models proceed essentially as described for the *gen-2bridge* model, with an reaction energy profile parallel to and some 10 kJ mol^{-1} below that found earlier (see Table 1). The three-bridge models are more rigid owing to the additional Cr—O ester linkage to the support and as a consequence, their potential energy surfaces do not possess local minima corresponding to any ethylhydridochromium(V) complexes. Hence oxidative addition of ethane is not likely to take place at such sites. This is further elaborated in the Discussion section.

Table 1. Thermodynamic parameters at 500 °C for C—H activation by oxidative addition on three models of the DeRossi site (values are given in kJ mol^{-1} relative to the asymptote of the unreacted cluster and gaseous ethane) $C_2H_6 + Cr^{III} \rightarrow (C_2H_5)(H)Cr^{V}$

	gen-2bridge			*(100)-2bridge*	$Cr(OH)_3$
Model	ΔE_{elec}	ΔH	ΔG	ΔE_{elec}	ΔE_{elec}
MECP	161	140	262	147	147
TS	166	162	283	158	158
Product	161	164	279	151	153

β-Hydrogen transfer

Even for the two-bridge models, the primary products of C—H activation are unstable with respect to the reverse reaction of reductive elimination. According to Table 1, for the *gen-2bridge* model the electronic energy barrier of reductive elimination is a mere 5 kJ mol^{-1} and the enthalpic barrier actually vanishes. Completion of a dehydrogenation cycle therefore requires an immediate second reaction step. We have considered three candidates for this second step, all of which include removal of a β-hydrogen (H_β) from the ethyl ligand: transfer of H_β to the metal itself, transfer to an oxygen atom bonded to the metal or transfer to the hydrogen atom ligated to the metal.

β-Hydrogen transfer to chromium results in a dihydridochromium(V) surface complex and the release of ethene to the gas phase. The reaction is computed to be highly endothermic (94 kJ mol^{-1}) and does not appear a viable alternative. The electronic energy is computed to be 255 kJ mol^{-1} above that of the separated cluster and ethane.

Transfer of a β-hydrogen to the hydroxyl ligand of the *gen-2bridge* model to form water passes over an energy barrier at 134 kJ mol^{-1} above that of the reactant ethylchromium complex. We will see that the third alternative, β-hydrogen transfer to the hydrido ligand, to form H_2 and a di-σ-bonded ethene–chromium(V) complex, provides an easier route.

The primary product of the C—H activation step and hence the reactant of the present reaction step displays ethyl and hydrido ligands in axial and equatorial positions, respectively, in a pseudo-TBP structure. The $\angle HCrC_\alpha$ angle is narrow and H_β may approach the hydrido ligand only if the ethyl moiety is twisted to one side, to make the C—C bond become almost orthogonal to the Cr—hydrido bond. Although such a structure allows for close H—H contact, the carbon—chromium distance remains too long for bond formation between the β-carbon and chromium. This picture has emerged from numerous attempts to obtain a reaction path using relaxed linear transit (LT) models as well as relaxed two-dimensional scans of the potential energy surface with respect to the C_β—Cr and H_β—hydrido distances. Simultaneously scanning both of these critical distances, at $r(H_\beta$—H) and $r(C_\beta$—Cr) distances around 1.2 and 2.2 Å, respectively, the complex undergoes a stereochemical rearrangement which leads both ethyl and hydrido

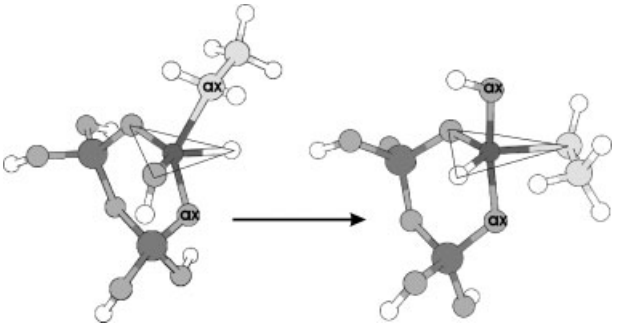

Figure 4. Stereochemical rearrangement subsequent to C—H activation on the *gen-2bridge* model. In the product, both the ethyl and hydride ligands occupy equatorial positions and the eclipsed configuration of the ethyl ligand is stabilized by β-agostic interaction with chromium

ligands to occupy equatorial positions. The $\angle HCrC_\alpha$ angle opens up from 63° in the reactant (see below) to 130°.

Prior to the rearrangement, the electronic energy exceeds 140 kJ mol^{-1} relative to the reactant ethylhydrido complex and 300 kJ mol^{-1} relative to the asymptote of the unreacted cluster and ethane. This is even more than the energy of the transition state of hydrogen transfer to the hydroxyl ligand. However, attempts to optimise a transition state for hydrogen transfer in this region have all failed, suggesting that the minimal energy path does not pass this way. Indeed, a route of notably lower energy was obtained as a two-segment reaction path, in which the steric rearrangement just described is a first and close-to-energy-neutral part, followed by the actual β-hydrogen transfer to the hydride.

In the early stage of the rearrangement, the reaction coordinate is dominated by dihedral angles (SiOCrL, L = OH, H and Et). Approaching the transition state, the reaction coordinate becomes mainly the $\angle HCrC_\alpha$ bond angle, which increases until the product configuration is reached (cf. Fig. 4). The reaction path does not comply with a Berry pseudo-rotation and the energy barrier is also higher than is commonly found for Berry transformations. According to Table 2, the activation enthalpy and free energy at the transition state of the stereochemical rearrangement amount to 220 and 347 kJ mol^{-1}, respectively, relative to the asymptote of separated cluster and ethane. The activation enthalpy of this reaction step (see below) is computed to 56 kJ mol^{-1}.

The most stable ethylhydridochromium complex displays the ethyl ligand in a staggered configuration. The eclipsed conformation shown in Fig. 4 lies only $\sim$20 kJ mol^{-1} higher in enthalpy. This structure accommodates a β-agostic interaction which makes it a natural starting point for the β-hydrogen transfer step.

Assisted by the agostic interaction, a β-hydrogen of the ethyl group may transfer to the hydrido ligand to form gaseous H_2 and a chromium(V)–cyclopropane surface complex in which ethylene is di-σ bonded to chromium. According to Table 2, the enthalpy and free energy at the transition state are 184 and 298 kJ mol^{-1}, respectively, relative to the asymptote of separated cluster and ethane. The activation enthalpy for the reaction, relative to the preceding non-agostic ethylhydrido complex, is 38 kJ mol^{-1}. The energy at the transition state of β-hydrogen transfer is therefore $\sim$40 kJ mol^{-1} lower than at the transition state of the preceding stereochemical rearrangement.

Table 2. Thermodynamic parameters at 500 °C for the reaction of ethene formation after C—H activation by oxidative addition on the *gen-2bridge* model [values are given in kJ mol^{-1} relative to the reactant asymptote (unreacted cluster + ethane)]

	ΔE_{elec}	ΔH	ΔG
***2**: Steric rearrangement of $(C_2H_5)(H)Cr^V$*			
Reactant	161	164	279
TS	224	220	347
Non-agostic product	162	146	268
β-Agostic product	163	166	292
***3**: β-H transfer $\rightarrow (C_2H_4)Cr^V + H_2$*			
TS	187	184	298
Product	149	119	137
***4**: Ethylene desorption $\rightarrow Cr^V + C_2H_4 + H_2$*			
MECP	160	123	131
π-Complex	131	104	99
Product	158	137	31

Dehydrogenation

The catalytic site may be regenerated by desorbing ethene from the chromium(V)–cyclopropane complex, thus completing the catalytic cycle. A complete mechanism of dehydrogenation is presented in Fig. 5 in terms of optimized stationary structures for the *gen-2bridge* model. The corresponding reaction enthalpy and free energy profiles are plotted in Fig. 6, with thermodynamic parameters for each of the elementary reaction steps given in Tables 1 and 2.

The four reaction steps shown in Fig. 5 include C—H activation (**1**), stereochemical rearrangement (**2**), β-hydrogen transfer (**3**) and ethene desorption (**4**). The desorption step involves spin flip at chromium to transform the di-σ-bonded ethene–chromium complex into a quartet $(—O)_2CrOH$ species with a π-bonded ethene. The crossing point (MECP) of the reaction path from the doublet to the quartet potential energy surface has been determined at an average Cr—C bond length of 2.20 Å and a C—C distance of 1.39 Å. These values are much closer to the geometry of the di-σ-bonded complex than that of the π-bonded ethene complex and the energy of the MECP is also very similar to the former.

The coordination enthalpy of the resulting ethene π-complex is only 33 kJ mol^{-1}, consistent with an almost unperturbed C—C bond length in ethene of 1.35 Å. Desorption of ethene is therefore favoured by entropy, resulting in a free energy change of -68 kJ mol^{-1} at 500 °C.

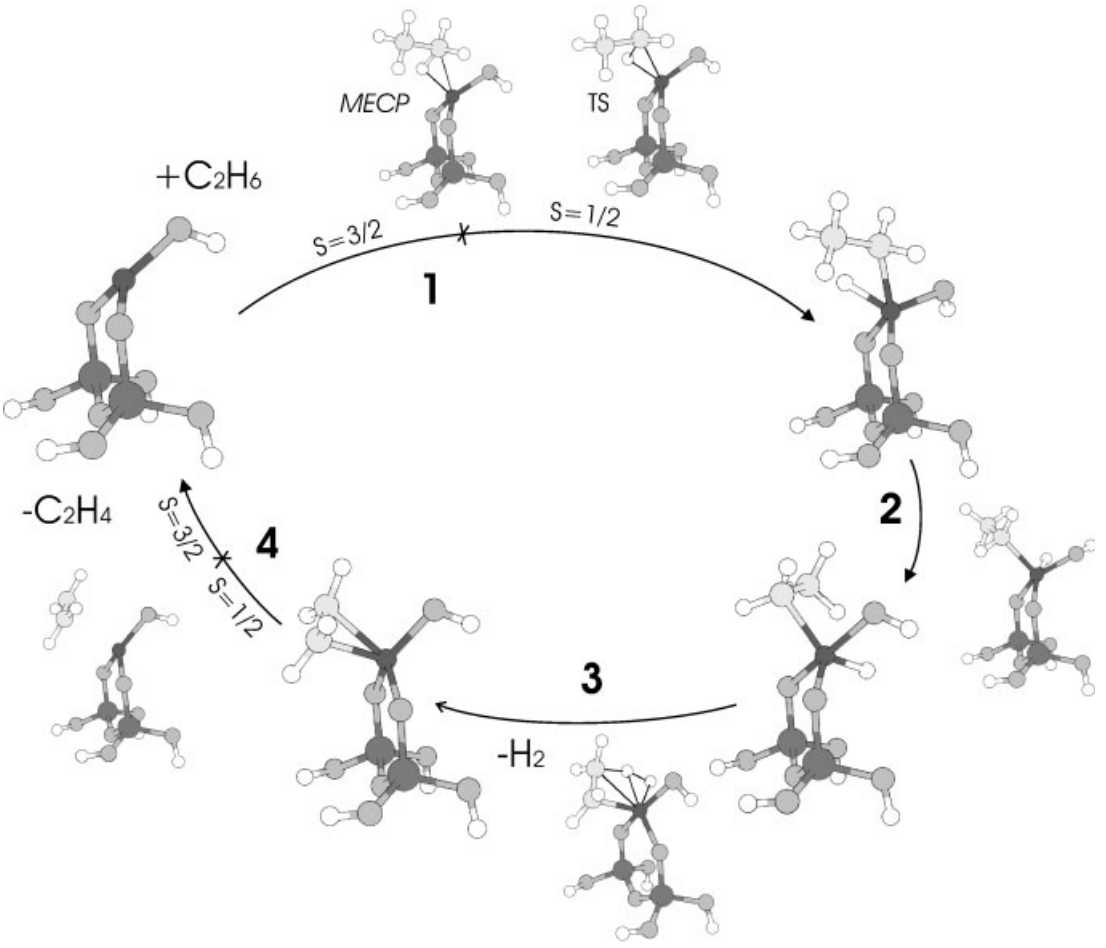

Figure 5. Optimized stationary structures for the catalytic dehydrogenation reaction of ethane over the *gen-2bridge* model catalyst. The reaction steps are (**1**) oxidative addition of ethane, (**2**) stereochemical rearrangement, (**3**) β-hydrogen transfer to hydride with subsequent loss of H_2, (**4**) spin-flip in the chromium(V)–cyclopropane complex, with subsequent loss of C_2H_4. Spin-crossover in reactions (**1**) and (**4**) is indicated by crosses on the arrows representing the reactions

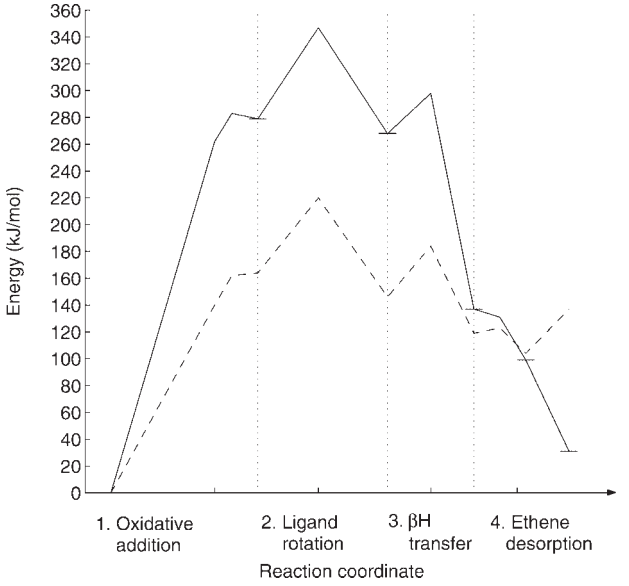

Figure 6. Profiles of the enthalpy (dashed line) and Gibbs free energy (full line) for the catalytic reaction of dehydrogenation of ethane via oxidative addition over the *gen-2bridge* model

From Fig. 6, the transition state of the stereochemical rearrangement step may be identified as the highest point on both the enthalpy and the free-energy reaction profiles for the overall dehydrogenation reaction.

The same mechanism of dehydrogenation has been examined for the *(100)-2bridge* and $Cr(OH)_3$ models. The electronic energies for all important stationary states are given in Table 3. The reaction energy profiles obtained for the *(100)-2bridge* and $Cr(OH)_3$ models are similar to that obtained for the *gen-2bridge* model. On all three models, the favoured route to β-hydrogen transfer was found to include stereochemical rearrangement. The electronic energies at the corresponding transition states are about $220\,kJ\,mol^{-1}$ for the *2bridge* models, with a lower energy of $196\,kJ\,mol^{-1}$ for $Cr(OH)_3$. This suggests that surface restraints contribute $\sim 20\,kJ\,mol^{-1}$ to the reaction barrier. Only for the β-hydrogen transfer reaction is the barrier markedly higher for the *(100)-2bridge* than for the *gen-2bridge* model (see Fig. 7). This is probably a result of poor β-agostic interaction with chromium, owing to the wider angle defined by the bridging oxygens and chromium. For both the

Table 3. Electronic energies for the reaction of ethene formation after C—H activation by oxidative addition (energies are given in kJ mol^{-1} relative to the unreacted cluster and ethane)

	Model		
	gen-2bridge	*(100)-2bridge*	$Cr(OH)_3$
***2**: Steric rearrangement of $(C_2H_5)(H)Cr^V$*			
Reactant	161	153	151
TS	224	221	196
Non-agostic product	162	166	179
β-Agostic product	163	—	177
***3**: β-H transfer $\rightarrow (C_2H_4)Cr^V + H_2$*			
TS	187	218	196
Product	149	147	138
***4**: Ethylene desorption $\rightarrow Cr^{III} + C_2H_4 + H_2$*			
MECP	160	170	175
π-Complex	131	151	149
Product	158	158	158

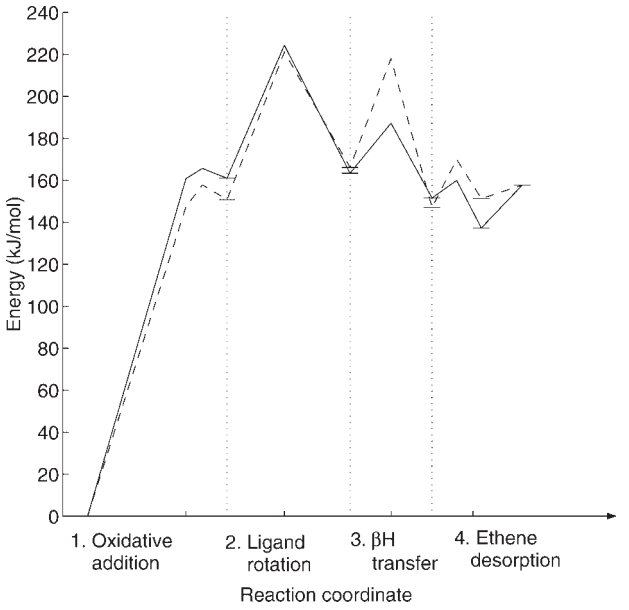

Figure 7. Electronic energy profiles for the reaction of dehydrogenation initiated by oxidative addition. The profiles correspond to the *gen-2bridge* (full line) and *(100)-2bridge* (dashed line) models

(100)-2bridge model and $Cr(OH)_3$, the transition states of the stereochemical rearrangement and the β-hydrogen transfer step are equally high in electronic energy. According to Table 2, the entropy loss is larger in the first of these two elementary reactions and this makes the stereochemical rearrangement the bottleneck of the overall dehydrogenation reaction for all the three DeRossi-type models examined.

DISCUSSION

The three-bridge models do not seem to offer any stable ethylhydridochromium(V) complexes, hence oxidative addition of ethane is not likely to take place at such sites. On the other hand, the models have previously been found to support C—H activation by σ-bond metathesis. This involves cleavage of a Cr—O bond and formation of a chromium–ethyl bond and a silanol moiety. A mechanism of dehydrogenation based on such a reaction was proposed in the literature[2,24] and studied theoretically in Ref. 23. In addition to the C—H activation step, it involves formation of ethene through β-hydrogen transfer to chromium, giving a hydridochromium complex and release of H_2 under reformation of the Cr—O bond. Strain in the *(111)-3bridge* model resulted in a low C—H activation energy of 80 kJ mol^{-1}, but also makes closure of the catalytic cycle a highly unlikely event. On the nearly unstrained *(101)-3bridge* model the C—H activation energy increased to 160 kJ mol^{-1}, but now the dehydrogenation cycle appeared viable. β-Hydrogen transfer turns out to be the rate-determining step with the enthalpy and free energy of activation estimated as 240 and 350 kJ mol^{-1}, respectively, These values seem too high to sustain catalysis at 500 °C.[23]

Based on the present computations, C—H activation by oxidative addition appears possible on DeRossi-type species, i.e. on CrOH moieties bonded to the surface via two oxygen bridges. The activation energy computed for this initial step is $\sim$160 kJ mol^{-1}. However, since the ethylhydridochromium complex is unstable with respect to reductive elimination, the subsequent step towards dehydrogenation must proceed immediately. The bottleneck of C—H activation by oxidative addition is therefore better represented by the transition state of the stereochemical rearrangement. Furthermore, as the free energy at this point represents the highest point along the reaction path of dehydrogenation, C—H activation emerges as rate determining in the dehydrogenation process. The computed enthalpy and free energy of activation are 220 and 347 kJ mol^{-1}, respectively.

The overall activation energy for dehydrogenation based on oxidative addition is therefore fairly high and on a level with that of the σ-bond metathesis reaction on unstrained three-bridge species. In addition, the reaction depends on two crossings between spin potential surfaces. For reactions of FeO^+, spin cross-over probabilities as low as 10^{-2}–10^{-3} have been obtained,[43] and even if the probability for a transition metal-mediated two-state reaction may be significantly increased by the exact makeup of the complex,[44] the actual probability of the present reaction is likely to be notably lower than unity. More importantly, the rotational segment of C—H activation, i.e. the stereochemical rearrangement step, puts severe constraints on the angular momentum of the reacting alkane molecule. The steric factor in the reaction cross-section is therefore likely to be small, further reducing the pre-exponential factor in the rate constant.

On DeRossi-type species, C—H activation by σ-bond metathesis, with transfer of hydrogen to the hydroxyl

ligand, gives water which is likely to desorb.[23] Reformation of the DeRossi site under release of H_2, as described above, is therefore unlikely. However, the surface site is stabilized as an ethylchromium complex and this species supports catalytic dehydrogenation through cyclic repetition of (i) β-hydrogen transfer to give a hydridochromium complex and (ii) C—H activation and H_2 release by σ-bond metathesis.[23] The computed activation energy for this mechanism of dehydrogenation is $<100\,kJ\,mol^{-1}$, with respect to the combined energy of the hydridochromium complex and gaseous ethane.[23] Moreover, the activation energy associated with forming the initial ethylchromium complex was computed as $130\,kJ\,mol^{-1}$,[23] which is significantly lower than that computed here for the C—H activation step according to oxidative addition.

CONCLUSIONS

Quantum chemical cluster models of Cr(III)–silica sites have been used to study C—H activation of ethane by oxidative addition. The reaction involves a formal double oxidation of chromium and whereas most of the actual activation of the C—H bond takes place on the quartet spin potential energy surface of Cr(III), the transition state and the ethylhydridochromium(V) product are located on the doublet energy surface. The product is unstable with respect to the back-reaction and completion of a dehydrogenation cycle requires that β-hydrogen transfer must take place in the extension of the C—H activation step. On sites where chromium is linked to the silica surface through two oxygen bridges, the preferred mode of β-hydrogen transfer is via a stereochemical rearrangement of the ethylhydridochromium(V) complex, followed by hydrogen transfer to the hydrido ligand with release of H_2. This leaves the complex as chromium(V)–cyclopropane.

On sites where chromium is linked to the silica surface through three oxygen bridges, we have not been able to optimize any ethylhydridochromium(V) structure and C—H activation according to oxidative addition seems to be excluded.

The reactant two-bridge (DeRossi) site may be regenerated from chromium(V)–cyclopropane by desorption of ethene. This concludes a catalytic cycle for dehydrogenation, involving the following reaction steps: (i) oxidative addition of ethane followed by immediate stereochemical rearrangement, (ii) β-hydrogen transfer to hydride with subsequent loss of H_2 and (iii) reductive elimination of ethene from chromium(V)–cyclopropane. The kinetic bottleneck of this reaction mechanism is given by the first step, which is associated with C—H activation but more precisely with the transition state of the rearrangement step. The computed enthalpy and free energy of activation are high, ca 220 and $350\,kJ\,mol^{-1}$, respectively, and close to the activation energies previously computed for a different mechanism of C—H activation, namely σ-bond metathesis, on specific three-bridge chromium sites.[23] Both of these seem inferior to a third mechanism of dehydrogenation, which involves C—H activation by σ-bond metathesis on a hydridochromium(III) species. The computed activation energy of the latter mechanism is $<100\,kJ\,mol^{-1}$,[23] and the two-bridge models investigated here may act as precursors to this more active species. C—H activation by oxidative addition thus seems to be an unlikely route to catalytic dehydrogenation for Cr(III)–silica catalysts.

Acknowledgement

We thank the Research Council of Norway (NFR) for financial support (KOSK 141953 431) and for a grant of computer time through the Programme for Supercomputing.

REFERENCES

1. Frey FE, Huppke WF. *Ind. Eng. Chem.* 1933; **25**: 54–59.
2. Weckhuysen BM, Schoonheydt RA. *Catal. Today* 1999; **51**: 223–232.
3. Weckhuysen BM, Bensalem A, Schoonheydt RA. *J. Chem. Soc., Faraday Trans.* 1998; **94**: 2011–2014.
4. DeRossi S, Ferraris G, Fremiotti S, Garrone E, Ghiotti G, Campa MC, Indovina V. *J. Catal.* 1994; **148**: 36–46.
5. Cavani F, Koutyrev M, Trifiro F, Bartolini A, Ghisletti D, Iezzi R, Santucci A, DelPiero G. *J. Catal.* 1996; **158**: 236–250.
6. Hakuli A, Kytokivi A, Krause AOI, Suntola T. *J. Catal.* 1996; **161**: 393–400.
7. Hakuli A, Harlin ME, Backman LB, Krause AOI. *J. Catal.* 1999; **184**: 349–356.
8. Weckhuysen BM, Verberckmoes AA, Debaere J, Ooms K, Langhans I, Schoonheydt RA. *J. Mol. Catal. A* 2000; **151**: 115–131.
9. Ghiotti G, Chiorino A. *Spectrochim. Acta, Part A* 1993; **49**: 1345–1359.
10. Airaksinen SMK, Harlin ME, Krause AOI. *Ind. Eng. Chem. Res.* 2002; **41**: 5619–5626.
11. Stahl SS, Labinger JA, Bercaw JE. *Angew. Chem. Int. Ed.* 1998; **37**: 2181–2192.
12. Siegbahn PEM, Crabtree RH. *J. Am. Chem. Soc.* 1996; **118**: 4442–4450.
13. Schröder D, Shaik S, Schwarz H. *Acc. Chem. Res.* 2000; **33**: 139–145.
14. Harvey JN, Poli R, Smith KM. *Coord. Chem. Rev.* 2003; **238**: 347–361.
15. Arndtsen BA, Bergman RG, Mobley TA, Peterson TH. *Acc. Chem. Res.* 1995; **28**: 154–162.
16. Niu SQ, Hall MB. *Chem. Rev.* 2000; **100**: 353–405.
17. Casty GL, Matturro MG, Myers GR, Reynolds RP, Hall RP. *Organometallics* 2001; **20**: 2246–2249.
18. Hall MB, Fan HJ. *Adv. Inorg. Chem.* 2003; **54**: 321–349.
19. Milet A, Dedieu A, Kapteijn G, van Koten G. *Inorg. Chem.* 1997; **36**: 3223–3231.
20. Whittlesey MK, Mawby RJ, Osman R, Perutz RN, Field LD, Wilkinson MP, George MW. *J. Am. Chem. Soc.* 1993; **115**: 8627–8637.
21. Xu X, Faglioni F, Goddard WA III. *J. Phys. Chem. A* 2002; **106**: 7171–7176.
22. Filippou AC, Schneider S, Schnakenburg G. *Angew. Chem. Int. Ed.* 2003; **42**: 4486–4489.
23. Lillehaug S, Børve KJ, Sierka M, Sauer J. *J. Phys. Org. Chem.* 2004; **17**: 990–1006.
24. Burwell RL, Littlewood AB, Cardew M, Pass G, Stoddard CTH. *J. Am. Chem. Soc.* 1960; **82**: 6272–6280.
25. Lillehaug S, Børve KJ. Working title: the role of the carrier oxide in Cr/oxide catalysts for dehydrogenation of ethane. Submitted for publication.

26. te Velde G, Bickelhaupt FM, van Gisbergen SJA, Fonseca Guerrax C, Baerends EJ, Snijders JG, Ziegler T. *J. Comput. Chem.* 2001; **22**: 931–967.
27. Fonseca Guerra C, Snijders JG, te Velde G, Baerends EJ. *Theor. Chem. Acc.* 1998; **99**: 391–403.
28. Baerends EJ, Autschbach JA, Bérces A, Bo C, Boerrigter PM, Cavallo L, Chong DP, Deng L, Dickson RM, Ellis DE, Fan L, Fischer TH, Fonseca Guerra C, van Gisbergen SJA, Groeneveld JA, Gritsenko OV, Grüning M, Harris FE, van den Hoek P, Jacobsen H, van Kessel G, Kootstra F, van Lenthe E, Osinga VP, Patchkovskii S, Philipsen PHT, Post D, Pye CC, Ravenek W, Ros P, Schipper PRT, Schreckenbach G, Snijders JG, Sola M, Swart M, Swerhone D, te Velde G, Vernooijs P, Versluis L, Visser O, van Wezenbeek E, Wiesenekker G, Wolff SK, Woo TK, Ziegler T. *ADF 2002.03 Computer Code*, 2002.
29. Vosko SH, Wilk L, Nusair M. *Can. J. Phys.* 1980; **58**: 1200–1211.
30. Perdew JP. *Phys. Rev. B* 1986; **33**: 8822–8824.
31. Becke AD. *Phys. Rev. A* 1988; **38**: 3098–3100.
32. Harvey JN, Aschi M, Schwarz H, Koch W. *Theor. Chem. Acc.* 1998; **99**: 95–99.
33. Harvey JN, Aschi M. *Phys. Chem. Chem. Phys.* 1999; **1**: 5555–5563.
34. Jensen VR, Børve KJ. *Organometallics* 1997; **16**: 2514–2522.
35. Jensen VR, Børve KJ. *J. Comput. Chem.* 1998; **19**: 947–960.
36. Ziegler T. *Chem. Rev.* 1991; **91**: 651–667.
37. Ziegler T. *Can. J. Chem.* 1995; **73**: 743–761.
38. Poli R, Harvey JN. *Chem. Soc. Rev.* 2003; **32**: 1–8.
39. Harvey JN. *Struct. Bond.* 2004; **112**: 151–183.
40. Espelid Ø, Børve KJ, Jensen V. *J. Phys. Chem. A* 1998; **102**: 10414–10423.
41. Jensen VR, Thiel W. *Organometallics* 2001; **20**: 4854–4862.
42. Frisch MJ, Trucks GW, Schlegel HB, Scuseria GE, Robb MA, Cheeseman JR, Zakrzewski VG, Montgomery Jr JA, Stratmann RE, Burant JC, Dapprich S, Millam JM, Daniels AD, Kudin KN, Strain MC, Farkas O, Tomasi J, Barone V, Cossi M, Cammi R, Mennucci B, Pomelli C, Adamo C, Clifford S, Ochterski J, Petersson GA, Ayala PY, Cui Q, Morokuma K, Malick DK, Rabuck AD, Raghavachari K, Foresman JB, Cioslowski J, Ortiz JV, Baboul AG, Stefanov BB, Liu G, Liashenko A, Piskorz P, Komaromi I, Gomperts R, Martin RL, Fox DJ, Keith T, Al-Laham MA, Peng CY, Nanayakkara A, Challacombe M, Gill PMW, Johnson B, Chen W, Wong MW, Andres JL, Gonzalez C, Head-Gordon M, Replogle ES, Pople JA. *Gaussian 98, Revision A.9*. Gaussian: Pittsburgh, PA, 1998.
43. Danovich D, Shaik S. *J. Am. Chem. Soc.* 1997; **119**: 1773–1786.
44. Jensen KP, Ryde U. *J. Biol. Chem.* 2004; **279**: 14561–14569.